CANADA

DEPARTMENT OF
ENERGY, MINES AND RESOURCES
MINES BRANCH
OTTAWA

THE MECHANICS OF SUPPORT AND CAVING IN LONGWALL TOP-SLICING

D. F. COATES AND M. GYENGE

FUELS AND MINING PRACTICE DIVISION

Reprinted from the Proceedings of the Fourth Intl. Conference on Strata Control and Rock Mechanics, Columbia University, New York, May 1964. pp. 70-84

Reprint Series RS 20

Price 25 cents

Available by mail from the Queen's Printer, Ottawa,
and at the following Canadian Government bookshops:

OTTAWA
Daly Building, Corner Mackenzie and Rideau

TORONTO
Mackenzie Building, 36 Adelaide St. East

MONTREAL
Aeterna-Vie Building, 1182 St. Catherine St. West

or through your bookseller

A deposit copy of this publication is also available
for reference in public libraries across Canada

Price 25 cents Cat. No. M38-8/20

Price subject to change without notice

ROGER DUHAMEL, F.R.S.C.
Queen's Printer and Controller of Stationery
Ottawa, Canada
1966

The mechanics of support and caving in longwall top-slicing

D. F. COATES and M. GYENGE

Department of Mines and Technical Surveys, Ottawa, Canada

INTRODUCTION

The work described in this paper was done as part of a cooperative research project with a mining company that was in the process of examining various underground mining methods. It was decided, in view of the development of modern equipment, to conduct an experimental operation in top-slicing using a longwall configuration.

In brief, a mat of timber and chain-link mesh was to be laid in an initial slice immediately under the pit waste that had been drawn down to this level by former block-caving operations. (See Figure 1.) The mat would then be supported for subsequent slices by friction props. (See Figure 2.)

Basic information was needed on the distribution of stress around the mine opening together with its effects on the prop loads, the stability of the face, the stability of the underdrift, and the caving in the tail area. It was anticipated, that all of these technical factors could have some influence on operating efficiency and, in particular, that the handling of props would greatly influence costs. The mobility of lightweight props would do much to make the mining method economically feasible. On the other hand, the need for heavy props, and any difficulties in moving them, would make the method too costly for iron-ore mining. It was also considered possible that the increased stress in the longwall face resulting from arching over the mine opening might cause some caving in blast holes in this incompetent ore. This concentration of stress being transmitted below the mining area conceivably would, in addition, affect the stability of the conveyor drifts under the slice.

EXPERIMENTAL PROGRAM

Theories of Stress Distribution

It was assumed that the yielding of the props would induce arching action as shown in Figure 2(a) in the overlying ground. This arching action would result in some portion of the weight of the overlying ground being carried out into the abutment zones. To calculate the average vertical pressure that would remain at the bottom of this subsiding zone (i.e., in the roof ground over the mining opening), the theory originally developed for pressures in deep bins and subsequently modified for arching in cohesive ground was used.[1] For the two-dimensional case or where the width of the arching zone is small with respect to its length, this theory gives the following formula

$$\sigma_v = \frac{b(\gamma - 2c/b)}{2k\tan\phi}\left(1 - e^{-k\tan\phi\cdot 2z/b}\right), \qquad (1)$$

where

- σ_v = the average vertical pressure that would be applied in this case to the mat over the mining opening,
- b = the span of the subsiding zone,
- γ = the density of the overlying ground,
- c = the cohesion of the overlying ground,
- ϕ = the angle of internal friction of the overlying ground,
- k = the coefficient of lateral earth pressure acting at the vertical boundaries of the subsiding zone,
- z = the depth of material above the mat, and
- e = the base of natural logarithms.

* Head, Mining Research Laboratories and ** Senior Scientific Officer, Mining Research Laboratories, Fuels and Mining Practice Division.

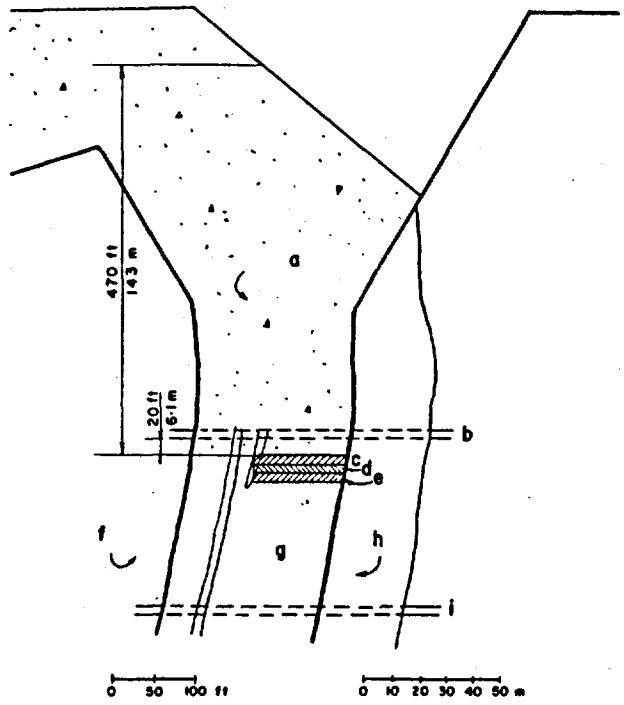

KEY

a = Pit waste	e = Third slice
b = 700 Level	f = Hangingwall ash rock
c = First slice	g = Ore
d = Second slice	h = Footwall paint rock
	i = 900 level

FIGURE 1 *Cross-section of mining zone.*

It is assumed in this theory that the vertical pressure σ_v is uniform. Although it can be expected that the actual pressure will be greater in the center of the area than at the edges, no theory has yet been established to predict the distribution of pressure. In addition, the coefficient of lateral earth pressure at the sides of the subsiding zone k is assumed to be constant. On the basis of experiments which showed that the value of k increased on the centerline from about unity at the bottom of the subsiding zone to a maximum of about 1.5 at an elevation approximately equal to the width above the bottom, it was concluded that an average value of 1 should be used.[1] However, this theory ignores the fact that the value of k that is applicable in these calculations is that which occurs at the sides of the subsiding zone. Once it is assumed that the surfaces of incipient sliding are these vertical boundaries, the authors believe that the ratio of horizontal to vertical stresses is determined by the necessary stress relations as shown in Figure 2(b). From this analysis it follows that

$$k = \frac{\sigma_v - 2c\tan\phi}{\sigma_v - (1 + 2\tan^2\phi)}. \qquad (2)$$

This equation, as well as measurements on silos,[2,3] indicates that an average value of $k = 0.5$ is more appropriate.

From drained triaxial laboratory tests on recompacted ore and waste, it was judged that the appropriate strength parameters for predicting prop loads would be $c = 6$ psi (0.4 kg/cm²) and $\phi = 32°$. The average density of the overlying ground based on field density tests and laboratory compaction tests was assumed to be 150 pcf (2400 kg/m³) under caving action. The span of the subsiding zone b was based on observations of the mat action in the tail area of the first slice. The depth of the subsiding zone z was approximately 470 feet (143 meters). With these figures, equation (1) was used to calculate the vertical pressure on the mat:

$$\sigma_v = \frac{40(150 - 2 \times 6 \times 144/40)}{2 \times 0.5\tan 32°}.$$

$$(1 - e^{-0.5(\tan 32°)2 \times 470/40}).$$

$$\sigma_v = 6840 \text{ psf } (33\,400 \text{ kg/m}^2)$$

If the rows of props normal to the face are spaced 36 in. (91 cm) apart and we assume a simple beam distribution of load between the props and the abutments, the total ultimate load that would have to be carried by rigid props could be calculated. In Figure 2 the average distance between the face and the front props is shown as 7 feet (21 meters). This distance actually varied between 6 and 8 feet (18 and 24 meters). Also, in this figure the open distance behind the rear row of props is shown as nominally 12 feet (36 meters). The distance to the point where significant pressure between the mat and floor occurred could be much greater than 12 feet (36 meters), but 26 feet (78 meters) would be a typical distance. By using 8 feet (24 meters) for the face distance and 26 feet (78 meters) for the tail distance, the total load on three props then would be

$$P = 3 \times 6840\,(8/2 + 6 + 26/2)$$
$$= 471\,000 \text{ lb } (213\,500 \text{ kg}).$$

With 3 props in a row, the average prop load would then be

$$P = 471\,000/3 = 157\,000 \text{ lb}$$
$$= 78.5\,T \text{ (71.2 metric tons)}.$$

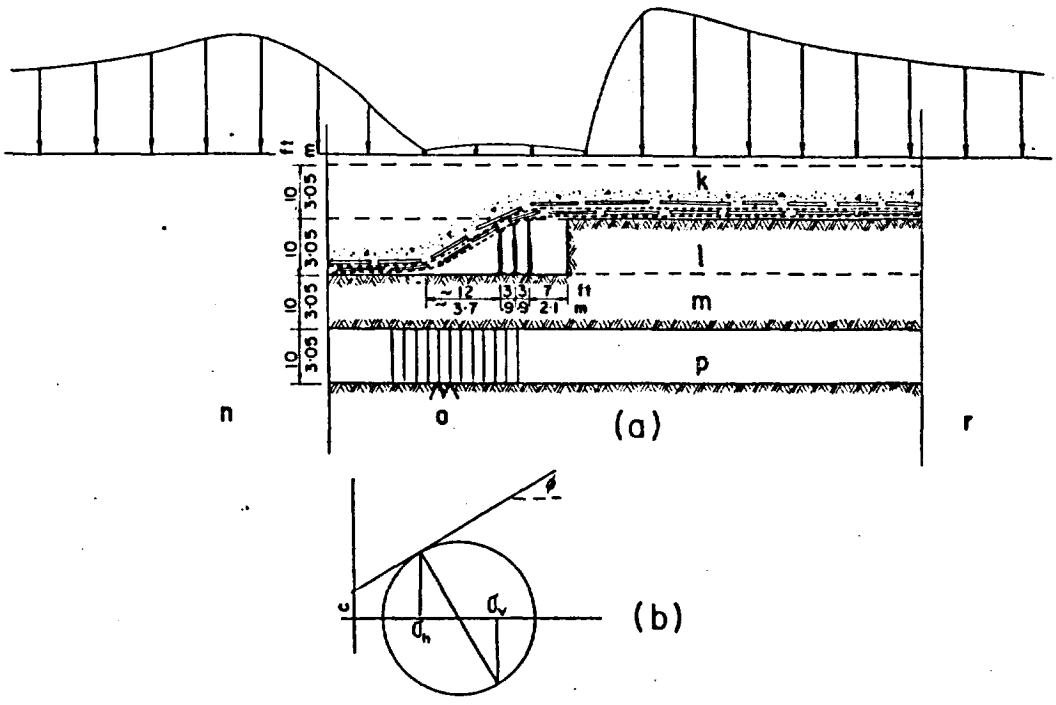

KEY

k	= First slice	n	= Footwall end of mat
l	= Second slice	o	= Hydraulic load cells
m	= Third slice	p	= Conveyor drift
		r	= Hangingwall end of mat

FIGURE 2 *Theoretical Section for analysis*
(a) Cross-section of longwall configuration
(b) Stress circle at edges of subsiding zone.

It is probable that the actual mat pressure would be a minimum at the longwall face abutment and a maximum in the area of the rear row of props. The distribution of prop loads in longwall mining under relatively competent layered roofs has indicated a similar pattern.[4] Using the average ratios of individual prop loads to total load found in coal mines, the following maximum and minimum prop loads were calculated.

$$\max P = 3 \times 78.5 \times 3/6 = 118\,T \text{ (108 metric tons), and}$$

$$\min P = 3 \times 78.5 \times 1/6 = 39\,T \text{ (35 metric tons).}$$

For the stability of the face of the underdrift, rough calculations were made of the possible maximum stresses that could exist at these locations; however, as these values were not based on any satisfactory theory they are not presented at this time. In addition, the variation of the strength of the undisturbed ore would make a failure prediction difficult even with an accurate calculation of stress.

The other aspect which could be analyzed theoretically and on which empirical observations obtained to either modify or confirm the theory, was the effect of the gob pressures on the mat itself. With props spaced approximately 36 in. (91 cm) apart in one row and with the rows spaced 36 in. (91 cm) apart, a two-way sag could be expected to occur in the mat. It was assumed that local arching in the gob would occur over the area between prop heads and that this two-way arching would in effect double the pressures that would be calculated using (1) derived for a two-dimensional case. It was also assumed that, with the intensive working of the ground immediately above the mat and with drying action, a conservative calculation should use $c = 0$. With the clear span $b = 24$ in. (61 cm), the follow-

ing pressure, using (1) and recognizing that the exponent of e is so large that the quantity in the bracket equals 1, was calculated $\sigma_v = (2 \times 150)/(2 \times 0.5 \tan 32°) = 480$ psf (2345 kg/m²). The total load carried by one strip of mat spanning between two props would then be $W = 480 \times 4 = 1920$ lb (870 kg).

To determine the result of this loading on the mat, one must initially assume that one layer only of the chain-link mesh is working. This mesh provided 0.174 sq in. (1.12 cm²) of cross-sectional area of steel wire per linear foot of mesh. It was assumed that a 1-foot (3-meter) wide strip of mesh extending between the heads of two props would carry the entire load calculated above. The sag of the mesh was assumed to be parabolic in shape and equal to 6 in. (15 cm). The equation based on the requirements for static equilibrium of a uniformly loaded parabolic membrane is as follows:

$$T = \frac{W}{2}\left[1 + \frac{1}{16}(B/D)^2\right]^{1/2}$$

where T is the tension in the membrane, W is the total load on the membrane, B is the span of the membrane and D is the sag at the center. Using this equation and dividing by the area of the mesh per linear foot, the stress, σ, in this working layer of mat was calculated as follows:

$$\sigma = \frac{1920}{2}\left[1 + \frac{1}{16}\left(\frac{2}{0.5}\right)^2\right]^{1/2} + 0.174 = 7.820 \text{ psi } (550 \text{ kg/cm}^2).$$

It can be seen that if these assumptions were valid then the mat would not be subjected to severe stresses in carrying the overlying ground. However, differential movements between props and shear stresses at the edges of prop heads could create more severe conditions than those for which the stress was calculated.

Prop Loads

Two methods were examined for measuring the loads on the props. An electrical-strain gage dynamometer was considered,[5] and Unidirectional Photostress Gages (Budd Instruments Ltd.) were also tested. Figure 3 shows the results of a test where the loads measured in a prop by both methods are compared to that indicated by the jack with which the load was applied. It can be seen that the agreement, except for low loads, between the stress

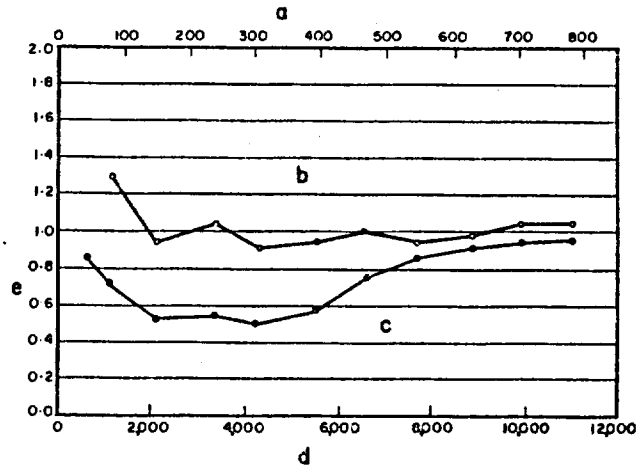

KEY

a = Stress level in prop (kg/cm²)
b = Average stress of Photostress / Average stress from jack load
c = Dynamometer load / Jack load
d = Stress level in prop (psi)
e = Ratio

FIGURE 3 *Comparison of Photostress and strain-gage dynamometer.*

in the steel calculated from the jack load and that measured with the Photostress was very good. In addition to the above test on the two methods of measurement, laboratory tests on the effects of time and underground trials on the effects of mining conditions resulted in the selection of the Photostress method.

It might be mentioned that the underground conditions of low temperature (50°F, 10°C) and high humidity affected the setting of the various cements that were tried in applying the Photostress to the steel. It was also found that applying and curing the gages in the laboratory and taking the prop underground resulted in a distortion of the fringes. Consequently, the complex procedure of applying the gages underground, waiting for the initial set, bringing the props up to the laboratory for final curing, and then taking the props back underground for use was finally adopted. Figure 4 shows the experimental top-slicing area and the various positions of the measuring props. It was expected that the total load on the props would be influenced by their position relative to the boundaries of the slice. To obtain a measure of these effects, Station I was selected to measure the influence of the hangingwall boundary. Station II was to give information about the effect of the side drift on the prop loads. Station III,

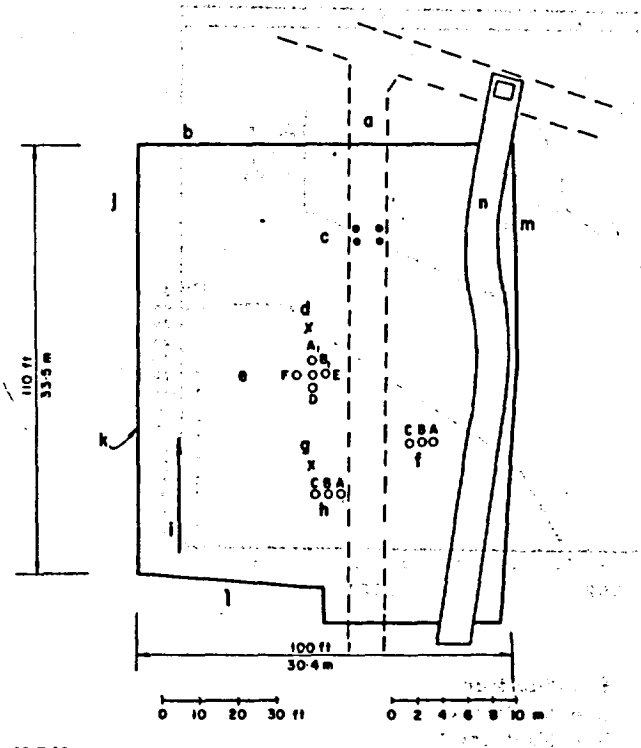

KEY

a	= Conveyor drift	h	= Station I
b	= Footwall	i	= Direction of mining in third slice
c	= Hydraulic load cells	j	= East
d	= Dynamometer "A"	k	= Edge of mat
e	= Station III	l	= Hangingwall
f	= Station II	m	= West
g	= Dynamometer "B"	n	= Side drift

FIGURE 4 *Plan of experimental installation.*

because of the absence of boundary effects, was expected to produce the maximum prop loads. Gage readings were taken hourly throughout the two working shifts with no measurements being available for the third shift.

Gob Pressures

To provide some information on the concentration of stress in the abutments of the arching gob (in other words, in the face and tail zones), prop dynamometers[5] were placed between two steel plates: 1-in. (2.54-cm) thick by 15-in. (39-cm) in diameter. After these cells were sealed in large rubber tubes, they were placed under the tail of the mat in locations as shown on Figure 4. Lead wires were carried to a convenient recording station either down a raise or through a drillhole to the underdrift.

Initially, these cells measured the buildup of pressure in the tail zone of the mat. When the slice in which they were installed was completed, another slice was mined out immediately below. This placed the cells in a position to measure the buildup of pressure as the face approached the instruments.

Set Loads

The drift that was located under the slices as shown in Figure 2(a) had its roof 20 feet (6 meters) below the floor of the first slice. The face of this mat-laying or first slice was parallel to the axis of the drift. As the face approached the station above the drift, an increase in ground pressure on the sets was manifest. The original wide-flange, rigid steel sets, after eight months of stability, started to fail when the face of the slice was 20 feet (6 meters) horizontally away. New, yielding arch sets were installed in this drift. When the face was still 10 feet (3 meters) away from the axis of the drift, four hydraulic load-cells[7] were installed under the legs of two of these sets.

These cells then monitored the increase in ground pressure on the sets as the top-slicing passed over the drift and showed the decrease in pressure as the slicing passed beyond it. These cells also measured the effects on the sets of being under the abutment zones of the subsequent longwall slice with the face moving normal to the axis of the drift as shown in Figure 2(a).

RESULTS

Prop Loads

Figure 5 is the graph of load and yield of prop B_1 located at Station III. Similar graphs were obtained for each of the prop positions shown in Figure 4. The yield recorded in Figure 5 is the slip in the friction lock of the yielding props. At the top of the graph, the letters *a*, *b*, *c* representing "Front," "Middle," and "Rear" indicate the relative position of the test prop with respect to the advancing mining face.

The load recorded in Figure 5 was obtained from the Photostress readings. These readings provided a measure of the strain at three locations around the circumference of the prop. This strain was then converted into stress, taking into account the possibility of plastic strain beyond the yield point. The average stress when multiplied by the cross-sectional area of the prop provided the load.

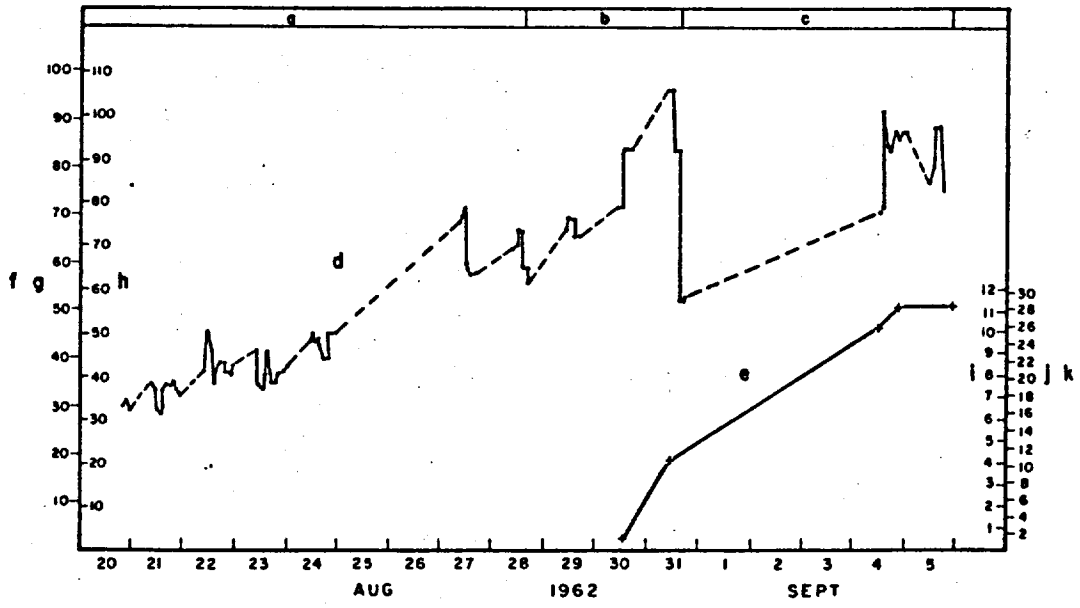

FIGURE 5 *Typical variation of prop load and yield with time.*

In Figure 6 the stresses in the wall of the prop are plotted to scale at the circumferential points at which the Photostress gages were cemented. These stresses occurred in prop *D* at Station III at different periods of time with (*K*) and (*L*) occurring when the prop was in the middle position, and (*M*) and (*N*) when the prop was in the rear position. The angle indicates the direction of the maximum stress in the prop wall.

Figure 7 shows the average load and yield for the props at Station III. These averages are of the three props for each working shift after installation.

Gob Pressure

Figure 8 shows the results of the readings for the two dynamometers that were set under the tail of the mat. As previously explained, these cells measured the gob pressures that occurred behind the face as the waste caved. They also measured the gob pressures as the face approached during the mining of the next slice down.

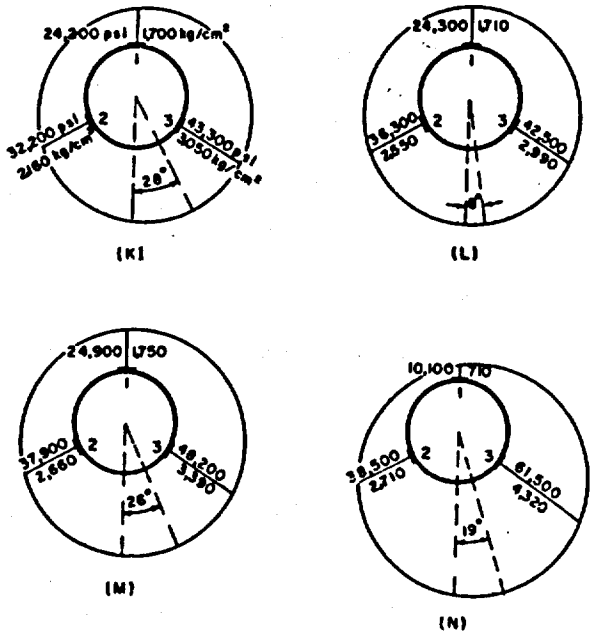

FIGURE 6 *Typical stress distribution in a prop.*

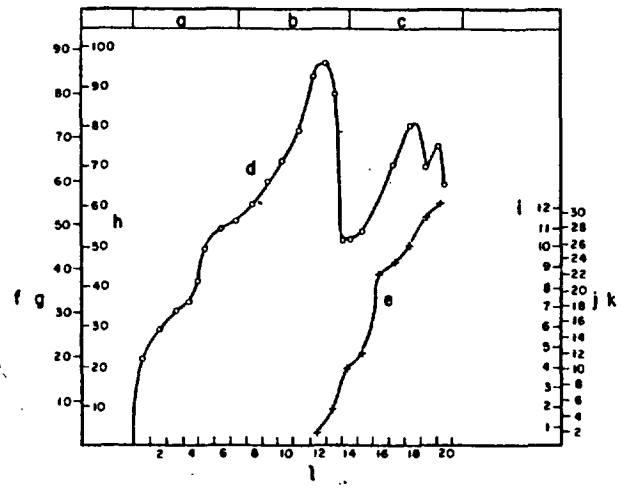

FIGURE 7 *Average prop load and yield curves for Station III.*

As these pressures are both a function of time and distance from the face, the information is not easily presented on a two-dimensional graph. Consequently, since Figure 8 shows pressure versus time, the face distance for the two cells are also plotted in Figure 9 so that the zones of pressure with respect to the face can be seen.

As mentioned, the dynamometers which measured the gob pressures used electrical-strain gage transducers. It was found during the four to seven months that these cells were in operation that the strain gages drifted. The total drift was determined by a final reading on the dynamometers when they had been relieved of all pressure. To correct the readings, it was assumed that this drift was a viscous reaction and consequently was proportional to time and the strain level. The readings shown in Figure 8 are the result of applying a correction based on this assumption to the original bridge readings.

Set Loads

Figure 10 shows the variation of pressure in the hydraulic load-cells under one of the instrumented sets. These pressures are also a function of time and distance from the mining face in the slices above. The pressure is plotted against time with notes made on the distance to the face at significant points. The pressures recorded by these load-cells were affected by the slicing operation in the two lifts above the drift; the first slice left a 20-foot (6-meter) pillar over the drift, and the second slice left a 10-foot (3-meter) pillar. It might be repeated (Figure 4) that the face of the first slice traveled from east to west and was thus parallel to the axis of the drift. The second slice traveled from footwall to hangingwall with the line of the face thus being perpendicular to the axis of the drift.

DISCUSSION

Prop Loads

Ultimate Loads. Ideally the load-time curve of Figure 6 should consist of a vertical line from the origin to the load required to activate the slip lock (nominally 40 tons, 36 metric tons) and then a horizontal line at this yield load. The ideal curve would have this shape since, theoretically, time is ignored for the transmission of elastic stresses and the slip lock should act as a constant yield point.

If it is recognized (although there is no theory relating these parameters) that the mobilizing of the plastic resistance of the ground is a time-consuming process (i.e., one requiring a certain amount of working of the ground), then the ideal load-time curve would consist of a sloping line starting from the origin indicating a uniform buildup of load during some finite rise time until the yield load was reached when the curve would become horizontal. In addition, the curve of deflection or yield of the prop versus time would then start at the time that the yield load on the prop was reached.

The actual curves depart greatly from this description of the ideal case. This departure arises from the dependence of the prop load on the initial load set by the placing jack, on the variation of yield load with time on any one prop, on the dependence of the yield load on deflection and deformation of the prop, and on the nonideal properties of the ground.

Possibly one of the most significant mechanisms influencing the prop loads is the effect of the load acting eccentrically to the head. This causes the friction lock to bind, thus inhibiting the slip which is designed to prevent excess pressures from building up. Figure 11 is a photograph of friction props supporting the chain-link mat. It can be seen here

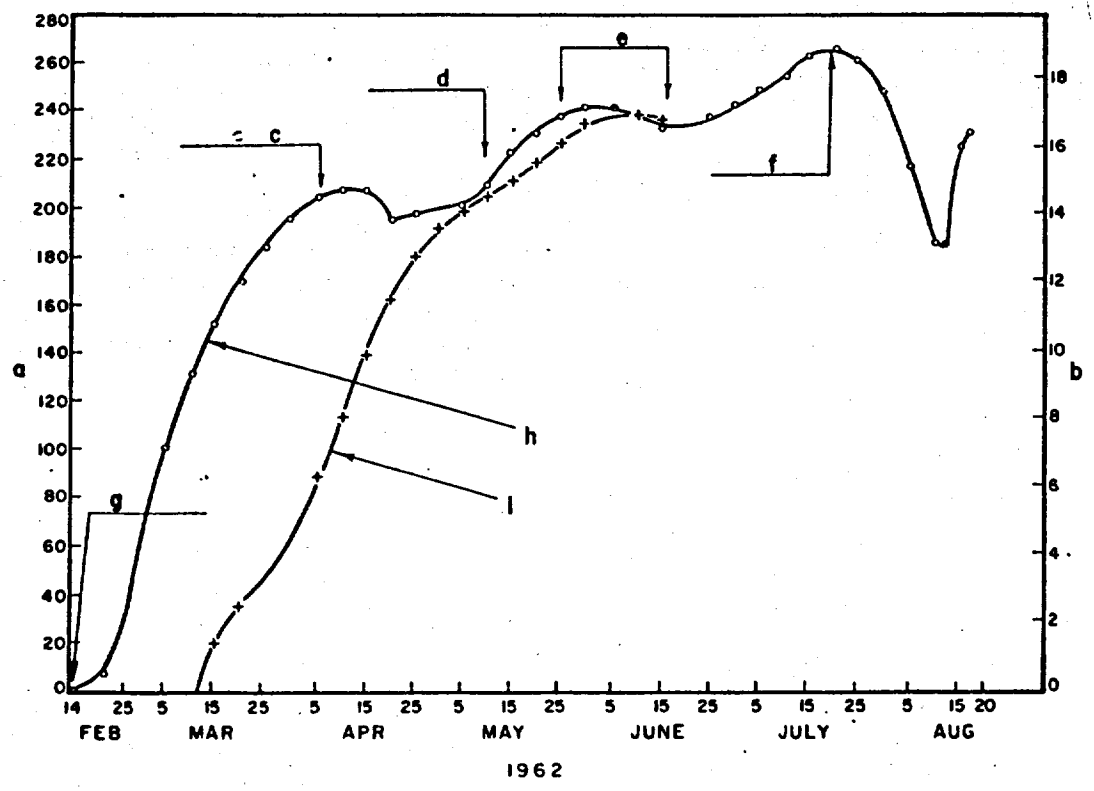

KEY

- a = Pressure in psi
- b = Pressure in kg/cm²
- c = Second slice completed; face 60 feet (18 meters) from Dynamometer "A", 30 feet (9 meters) from Dynamometer "B"
- d = Third slice started, face advancing towards and 60 feet (18 meters) from Dynamometer "A", 30 feet (9 meters) from Dynamometer "B"
- e = No advance of face
- f = Face 16 feet (5 meters) from Dynamometer "A"
- g = Face receding and 20 feet (6 meters) from Dynamometer "A"
- h = Dynamometer "A"
- i = Dynamometer "B"

FIGURE 8 *Variation of gob pressure with time.*

that the loads are unlikely to be applied vertically and along the axis of the prop. Figure 12 shows photographs of damaged props resulting from eccentric loading; figure 12(a) is a buckled section of the lower half of a Stahlunion prop, and Figure 12(b) is a bent Huwood prop.

The many cases that were measured where yielding of the prop did not occur give some indication of the ultimate loads that would occur if rigid props were used. These ultimate loads can be compared with the loads predicted by theory assuming rigid props. By examining all of the curves represented by Figure 5 for the periods where no yielding occurred, the ultimate loads for Station III were found to be of the order of 75 tons (68 metric tons). The calculated average load of 78.5 tons (71 metric tons) suggests that the arching theory with the authors' modifications is a good representation of the actual ground reaction.

The orders of magnitude of the ultimate loads in Stations I and II were lower than that for Station III. This is to be expected as a result of the nearness in each case of the boundary where shear stress would transfer the major part of the vertical load in

the immediately adjacent slice zone into the abutments. Furthermore, these positions could not be expected to be described by the theory because only the two-dimensional case is covered (i.e., end affects are not included).

It might be expected that these ultimate loads would be affected by the movement of adjacent props. Examination of the schedule of prop movements with the record of load on the test props indicate that the movement of adjacent props has little influence. At most, there seems to have been some decrease in the measured loads as a result of moving adjacent rear row props into the front row. It might also be expected that blasting on the face would affect the ultimate measured prop loads. This could occur either from the increase in span that is created or from simply the jarring of the ground in the back into a situation requiring additional deformation to develop the internal strength of the gob. Examination of the schedule of blasting adjacent to the measuring stations indicated that the effects on the prop loads were small. Consequently, any vibration effects on the overlying ground would seem to be insignificant, and the effect of the increased span might require several days to develop, which would tend to obscure any particular relationship between blasting and loads.

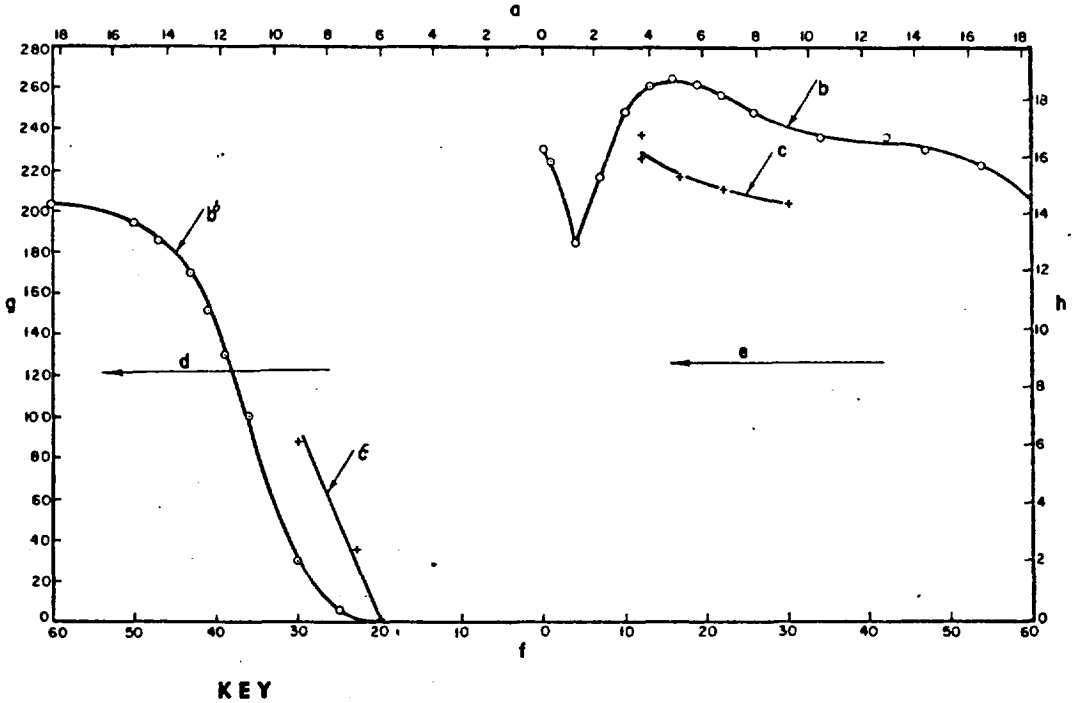

KEY

- a = Distance from face in meters
- b = Dynamometer "A"
- c = Dynamometer "B"
- d = In second slice the face moved toward dynamometers
- e = In third slice the face moved toward dynamometers
- f = Distance from face in feet
- g = Pressure in psi
- h = Pressure in kg/cm²

FIGURE 9 *Variation of gob pressure with distance from face.*

At Stations I and II, the loads on the front props were less than the yield load (nominally 40 tons, 36 metric tons). For the middle and rear positions at these stations, the props yielded, the loads being a function of the amount and rate of yielding as well as of time. Although there were many variables, it seems clear that at these Stations the ultimate loads on the props in the middle and rear positions would be greater than those in the front position.

At Station III, the loads on the front prop usually exceeded the nominal yield load. The measured loads after yielding would normally then be a function of the amount of yield, the rate of yield, and the time available for the buildup of load. Consequently, it is difficult to draw any firm conclusions regarding the relative loads between the front, middle, and rear positions. The differences between the front and middle positions may be the result of time rather than position. Figure 7 indicates, regardless of the causes, that the loads on the middle and rear props could be expected to be greater than those on the front row as was found for Stations I and II. Measurements in coal mines under stratified, uncaved roofs also showed loads that increased from front to rear.[4]

Time Effects. By examining those periods during which the face was not advancing, some indication can be obtained as to whether any creep occurred in the gob. From all the load-time curves, eight cases were found in which the load, aside from oscillations, increased as a result of time, and nine cases were found in which the load decreased. From this it can be concluded that the waste material does not have any viscous or creep properties. This is consistent with the laboratory testing that was done to examine this possibility.

The variation of load, both up and down, with time when other conditions were held constant must be due simply to the working of the roof material. It is reasonable to expect that as the face advances and causes changes in the stresses in the roof ma-

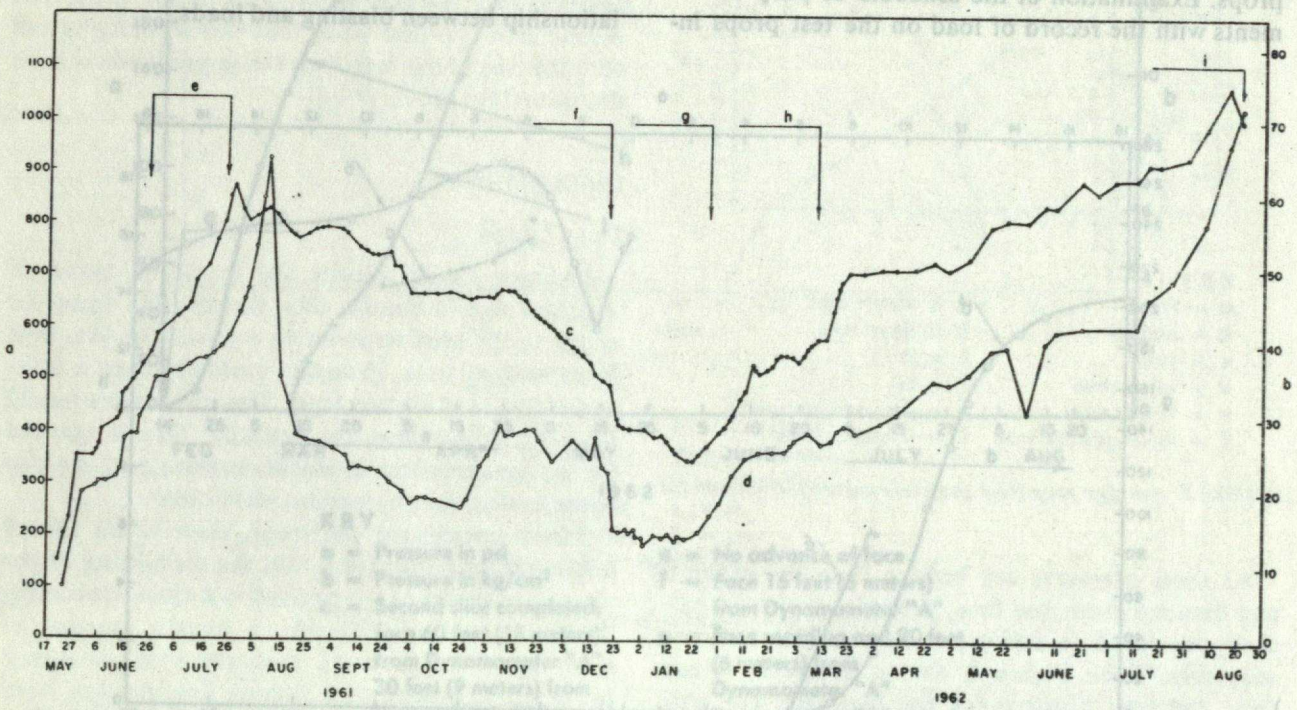

KEY

- a = Pressure in psi
- b = Pressure in kg/cm²
- c = Hydraulic load cell No. 2
- d = Hydraulic load cell No. 1
- e = First slice face over centerline of drift
- f = Second slice face over load cells
- g = Middle props over load cells
- h = Second slice face 65 feet (20 meters) beyond cells
- i = Third slice face 38 feet (12 meters) to load cells

FIGURE 10 *Variation of set loads in conveyor drift with time.*

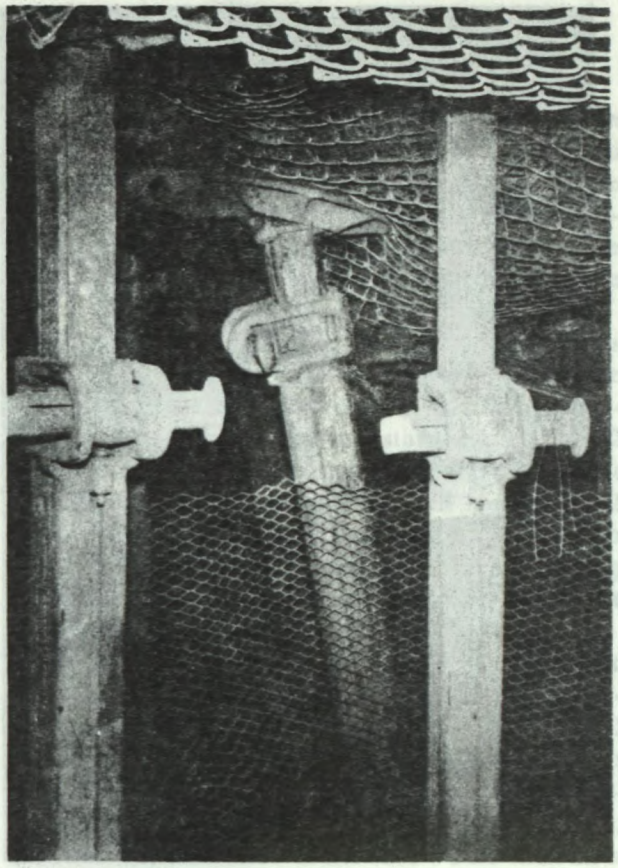

FIGURE 11 *Props supporting mat.*

terial the adjustment to these new stresses will require a certain amount of time before the roof works into a stable configuration. The actual fluctuation in load during these quiet periods is consistent with this mechanism.

It would be of interest to know how long it takes for the roof material to work itself into a stable configuration. There are too many variables affecting the prop loads to make an explicit analysis of this factor. One load curve suggested that the buildup of ultimate loads might take as little as one day, but the more common pattern that seems to emerge from an examination of these curves is that it might take up to ten days with seven days possibly being most common.

This effect of time can be thought of as a reduction in stress parameters (cohesion and internal friction) with the duration of stress. Consequently, if higher strength parameters would be governing the resultant loads on the props for periods of time for any one configuration less than about seven days, then it would be advantageous to adjust, if possible, the mining operations so that these higher strength parameters or lower resultant loads would only apply. Actually, the possibility of reducing the time for one mining cycle under full operating conditions was quite good.

Deformation Effects. It might be expected that the measured loads would show a decrease as the yield or slip in the friction lock of the props increased. The concept here would be that the prop would be relieved of its load. Alternatively, it might be expected that as the deformation increases the load would remain constant at the yield load for the prop.

Again, any attempt at correlation is complicated by the simultaneous action of other variables. In addition, the yield load for the props aside from any binding effects caused by eccentricity of loading did not seem to be constant. With no noticeable eccentricity the yield loads seemed to vary between 25 and 40 tons (23 and 36 metric tons). In some cases with obvious eccentricity, yielding did not occur until a load of 75 tons (68 metric tons) was reached.

By examining individual cases it seems that no reduction of load occurred with increasing yield. The action presumably was simple to prevent an increase in load from occurring. In addition, there seemed to be a rough correlation between load and cumulative yield as both increased with the passage of time. The normal explanation for the increase in the prop load would be that the probability of binding at the friction lock would increase with time thus creating an effective increase in the yield load.

Eccentricity of Loading. The magnitude and direction of the eccentricity of loading varied with the movement of the mat. This movement had an irregular component caused by the caving of the waste above the mat. The movement also had a regular component arising from the necessary kinematics of the mat associated with the vertical movement that results from the yielding of the props and the sinking of the mat towards the floor in the tail area. In some cases, the bending or leaning of the props was visible as shown in Figure 11. The analysis of the stresses at the various Photostress gages, as shown in Figure 6, showed that the angle of inclination to the face of the maximum stress changed in the same way as the visible bending in the prop changed.

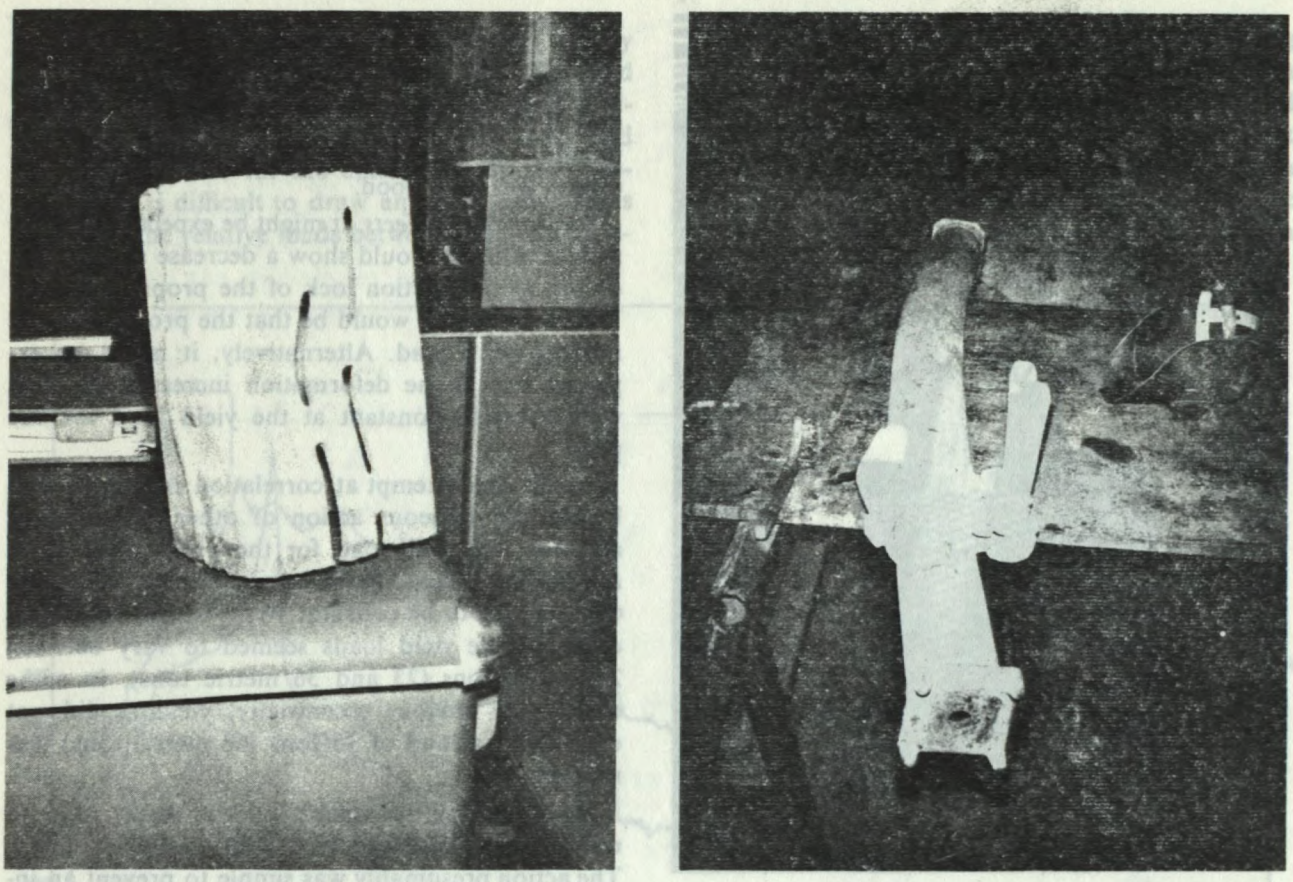

FIGURE 12 *Deformed props:* **a** *Stahlunion;* **b** *Huwood.*

Gob Pressure

By examining the data contained in Figure 8, it appears that the concentration of pressure in the face, as shown diagrammatically in Figure 2(a), extends for a distance of some 70 feet (21 meters). The tail area, which according to the arching theory should be subjected to an increased pressure of the same nature, seems to experience a stress concentration for more than 90 feet (27 meters) from the face or more than 70 feet (21 meters) from the nominal tail to floor contact of the mat.

From the magnitude of the pressure readings, it appears that the concentration of pressure in the face increases the normal gob pressure by a maximum of 90 percent. The pressure zone in the tail seems to increase the normal pressure by a maximum of 50 percent.

At the face, the pressure zone begins at a point several feet in from the face. This indicates that the face material relaxes or fractures before it is drilled and blasted. Some caving of blast holes did occur in this zone, which supports this postulate.

From the calculated dynamometer readings the average, normal gob pressure in this experimental block seems to have been about 174 psi (12.2 kg/cm^2). Calculations using (1) indicated that an average pressure of 148 psi (10.4 kg/cm^2) should have occurred. Considering the sources of inaccuracies that were found in the dynamometer readings (temperature effects, influence of length of lead wire, air humidity, and time of exposure of the strain indicator, as well as drift on the strain gages), this difference does not seem to be particularly significant.

Nowhere did the mesh in the mat seem to be overstressed. This was largely the result of the timber-bridging action rather than a proof of the validity of the predicted stress. The mesh was broken in a few locations from blasting in the face.

Set Loads

The failure of the original wide-flange sets in the underdrift as the face of the first slice approached the station of the drift provided immediate evidence that the concentration of face pressure was significant and was substantially transmitted through the 20 feet (6 meters) of horizontal pillar between the slice and the drift.

In Figure 10, the relief of pressure on the sets is quite clear and results from the face of the first slice passing over the drift between 27 July and 10 August. Furthermore, the decrease starting in cell No. 2 before cell No. 1 is consistent with the movement of the face in the direction from cell No. 2 to cell No. 1. This reduction in vertical ground pressure on the sets continued over a three-month period during which time the mat was being placed in this first slice.

After completion of the first slice, with the back caving down on the mat, the pit waste would be expected to arch over the mining area (100 × 110 feet; 30 × 33 meters), producing a reduction in vertical pressure from that existing on the undisturbed ore zone at that level. In the second slice, the stress concentration in the face would than be a concentration of this reduced vertical pressure. Consequently, the effects of the transmission of this stress concentration to the walls of the underdrift would be much less significant than the stress concentration in the face of the first slice.

As confirmation of this analysis of the ground stress regime, the load-cell readings preceding the passing of the face over the measuring station for the second slice showed no conspicuous rise. In addition, it should be noted that the load-cells would only record the effects of such stress concentrations if the stress was of sufficient magnitude to either significantly compress or fracture the ground around the drift. For the first slice this stress level was high enough to cause failure of the ground; whereas, in the second case the stress level, being lower, must also have been below the strength of the surrounding ground.

However, when the face of the second slice passed beyond the load-cell station, all of the load-cells immediately registered a drop in pressure (20 December in Figure 10). The vertical pressure on the sets started to rise again when the face was about 33 feet (10 meters) beyond the measuring station and the mat was just coming into contact with the floor. The cells farthest from the face, as would be expected, started to rise first. Measurements were continued during the mining of the first half of the third slice. However, as the floor elevation of the slice was at the elevation of the back of the drift, the readings had to be stopped when the face was still about 37 feet (11 meters) away from the measuring station. Consequently, no additional pertinent information regarding face pressures was obtained from these load-cells. The fact that the load-cells reading increased continually from the time of the completion of the second slice to the time immediately preceding their removal might be due to the working of the gob, possibly assisted by fairly heavy rains.

CONCLUSIONS

As a result of this research work a better understanding of the ground mechanics associated with top-slicing was obtained. The conclusions derived from this project are.

1 This increased understanding should make it possible, particularly on this property, to plan future operations, both in top-slicing and in other mining methods, with a better understanding of the ground reactions to be expected.
2 The order of magnitude of loads to be expected for unyielding props in top-slicing seems to be predictable from laboratory tests on the roof material. However, eccentricity of loading under a caving back with a reduction in capacity of props as a result of bending action should be expected. In this particular case, the props had a lower capacity than the maximum loads that developed.
3 The Photostress gage has several good features for measuring prop loads: low-cost, easy installation, and good reliability. However, it has some disadvantages: the same person should take all readings to avoid the variation of personal identification of fringes; it is possible to err when using the higher order fringes that have the same color; the calculation of strain from the actual readings is laborious; and the gages are sensitive to temperature changes.
4 The electrical-strain gage dynamometer was found to be somewhat unsatisfactory for measuring gob pressures because of the variation of readings that occurs with change in temperature, exposure to humid conditions, change in length of lead wire, and drift as a result of time and load.
5 The hydraulic load-cells used in this work are very satisfactory for measuring set loads over a period of at least a year.
6 The mat requirements for supporting gob pressure may be analyzed by considering the local arching that occurs between the heads of props. Rather low

structural requirements are found from this type of analysis, which does not include all the effects of importance. Thus, a large safety factor should be included in the design to account for such action as differential movements between prop heads, shear around prop heads, and blasting.

7 The sides of underdrifts in top-slicing may be fractured, depending on the size of the mining block and the depth of the drift below the slice, as a result of the stress concentration in the longwall face. If fracturing occurs, loads will be increased on the sets. The possibility exists of predicting when such increased loading is likely to occur.

ACKNOWLEDGEMENTS

It is a pleasure to acknowledge the important contributions to this work of the staffs of Steep Rock Iron Mines Ltd., and of the Rock Mechanics Laboratory in Ottawa as well as the particular work of Messrs. J. R. Helliwell and K. L. McRorie.

REFERENCES

1 TERZAGHI, K. *Theoretical Soil Mechanics*. New York: John Wiley and Sons, Inc., 1943.

2 JAKOBSON, B. On Pressure in Silos. *Proceedings of the Brussels Conference on Earth Pressure Problems 1958*. Vol. 1.

3 MOSS, E. The Design of a Raw Sugar Silo. *Inst. Civil Engrs. Conference on the Correlation Between Calculated and Observed Stresses and Displacements in Structures 1955*. Prelim. vol., paper No. 11, groups 2. Pp. 177–196.

4 SCHWARTZ, B. Measurement of Ground Pressure and of Movements at Longwall Faces in French Coal Mines. *Trans. Can. Inst. Mining Met.* (1954) 57: 259.

5 TYTE, L. and WYNNE, A. The Work of the Mining Research Establishment. *Trans. Inst. Min. Eng.* (1956) 116, Pt 2: 158.

6 ZANDMAN, F. *Photostress*. Soc. Nondestructive Testing Handbook. New York: Ronald Press Co., 1959.

7 PRICE, N. AND MAY, N. The Use of Pack Dynamometers. *Colliery Eng.* (Sept. 1960). 37: 379–382.